## Observation of the Superfluid Shapiro Effect in a <sup>3</sup>He Weak Link

R. W. Simmonds, A. Marchenkov, J. C. Davis, and R. E. Packard Department of Physics, University of California, Berkeley, California 94720 (Received 26 February 2001; published 26 June 2001)

We have studied the mass currents through a superfluid  ${}^{3}$ He Josephson weak link in the presence of an externally applied ac pressure modulation. Characteristic changes in the dc mass currents are observed whenever the superfluid Josephson frequency  $\omega_{J}$  is an integer multiple of the ac modulation frequency  $\omega$ . The measured dependencies of these current changes on ac pressure amplitude are in excellent agreement with theory describing quantum phase dynamics of superfluid  ${}^{3}$ He weak links. These results establish the superfluid analog of the superconducting Shapiro effect.

DOI: 10.1103/PhysRevLett.87.035301

In the original paper predicting the superconducting Josephson effect a test of the theory was outlined [1]. Josephson proposed that if, in addition to a dc voltage, a high frequency ac voltage is applied across a superconducting Josephson junction, the dc current will exhibit characteristic changes. Observation by Shapiro of these predicted phenomena [2] yielded the confirmation of the superconducting Josephson equations. For over thirty years much effort has been focused on searches for equivalent phenomena in superfluid weak links, both in [3,4] liquid <sup>4</sup>He and in [4–6] liquid <sup>3</sup>He. In this paper we now report the first observation of the *superfluid* Shapiro effect.

Josephson showed that superconductor-insulator-superconductor tunnel junctions pass a dissipationless electrical current I up to some critical value,  $I_c$ . The relationship of this current to  $\phi$ , the quantum phase difference across the junction, is given by

$$I = I_c \sin(\phi). \tag{1}$$

Furthermore, the reaction of  $\phi$  to a chemical potential  $\Delta \mu$  applied across the junction is given by

$$\frac{d\phi}{dt} = -\frac{\Delta\mu}{\hbar} \,. \tag{2}$$

Since in a superconductor,  $\Delta \mu = -2eV$ , application of a dc voltage produces current oscillations at the characteristic Josephson frequency  $\omega_J = 2eV/\hbar$ . When ac voltage oscillations of magnitude  $V_{\rm ac}$  are then superimposed at frequency  $\omega$ , characteristic changes in the dc current should occur when [7]

$$\omega_J = n\omega \tag{3}$$

for n = 0, 1, 2, 3, ... The magnitudes of these currents are given by

$$I_n = I_c |J_n(2eV_{\rm ac}/\hbar\omega)|, \qquad (4)$$

where  $J_n(x)$  is the cylindrical Bessel function of order n. When dc-biased superconducting weak lines are exposed to microwave radiation, they do indeed show the currents given by [2,8] Eq. (4). These phenomena, usually referred to as the Shapiro effect, provide the basis of much further research on practical applications of Josephson junctions, for example, as a voltage standard [9,10].

PACS numbers: 67.57.De, 74.50.+r, 85.25.Cp

Josephson weak links also exist for superfluid <sup>3</sup>He [11–13] where chemical potential differences are given by  $\Delta \mu = 2m_3P/\rho$ . Here P is an applied pressure difference,  $2m_3$  is the mass of a Cooper pair, and  $\rho$  is the density of the liquid. By analogy with Eqs. (1)–(4), under the combined application of a dc and ac pressure difference,  $P(t) = P_{\rm dc} + P_{\rm ac} \cos(\omega t)$ , new mass currents should be created when  $\omega_J = 2m_3P_{\rm dc}/\rho\hbar$  satisfies Eq. (3). The currents would then be given by

$$I_n = I_c \left| J_n \left( \frac{2m_3 P_{\rm ac} / \rho}{\hbar \omega} \right) \right|, \tag{5}$$

where  $I_c$  is the mass critical current of the weak link. In other words, Eq. (5) implies that the zero-pressure critical current (i.e., n=0) should be *reduced* proportional to  $J_0[(2m_3P_{\rm ac}/\rho)/(\hbar\omega)]$ , while for n>0 additional dc mass currents should appear proportional to  $J_n[(2m_3P_{\rm ac}/\rho)/(\hbar\omega)]$  when  $\omega_J=\omega,2\omega,3\omega,\ldots$ 

A superfluid weak link consists of a coherencelength-sized aperture connecting two superfluid reser-Superfluid <sup>3</sup>He is favored in the search for Josephson-like phenomena because for <sup>3</sup>He the coherence length  $\xi_3 \sim 100$  nm [14], while for <sup>4</sup>He  $\xi_4 \sim 0.1$  nm [15]. For the <sup>3</sup>He system, microfabrication technology using silicon-nitride membranes allows production [16] of nanoapertures with sizes on the order of  $\xi_3$ . We have fabricated a square array of 4225 holes in a nominally 50 nm thick membrane. The average aperture diameter is close to 115 nm and each aperture is separated from its nearest neighbor by 3  $\mu$ m. Equations (1) and (2) are directly validated at low frequencies for these microaperture arrays [12,13]. The question naturally arises: Is it possible to observe the Shapiro effect using a superfluid <sup>3</sup>He microaperture-array weak link? This experiment has been designed to answer that question.

Figure 1 shows a schematic diagram of our apparatus which has been described [11,12] elsewhere. It consists of an "outer" volume of superfluid, which houses a flat cylinder containing an "inner" volume of superfluid. Two flexible Kapton diaphragms form the top and bottom surfaces of this inner cylinder. Each diaphragm has a metallized surface and a corresponding electrode that

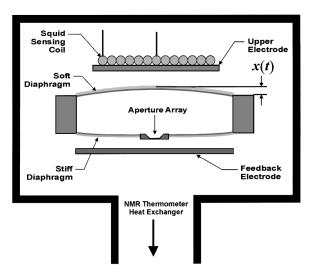


FIG. 1. A schematic diagram of the experimental apparatus.

allows the application of electrostatic pressures to it. The upper membrane is magnetically coupled to a superconducting dc-SQUID displacement transducer that registers its position [17]. The Si chip containing the microaperture array is glued to the center of the lower membrane. The cell can be cooled well below the superfluid transition temperature using a nuclear demagnetization cryostat. All experiments reported here were at zero ambient pressure and at a temperature where we have determined that the current phase relation is sine-like [13].

We control the value of  $P_{dc}$  using a feedback system with which we vary the electrostatic forces applied to the lower membrane so that the deflection of the upper membrane (our pressure gauge), and thus  $P_{\rm dc}$ , is held fixed [18]. We create the pressure  $P_{\rm ac}$  by applying an oscillating voltage to the upper electrode. These oscillations are at sufficiently high frequency that the feedback system ignores them. By knowing the amplitude of the applied voltage we can calculate the magnitude of ac pressure oscillations  $P_V$  applied across the fluid in the cell. Because the system in Fig. 1 is a hydrodynamic resonant circuit [19],  $P_V$  is not identical to  $P_{\rm ac}$ , the amplitude of pressure oscillations across the weak link. In fact,  $P_{\rm ac}=\alpha_n P_V$ , where  $\alpha_n$  represents the transfer function of the hydrodynamic system in Fig. 1. The value of the transfer function  $\alpha_n$  depends on the temperature T and on frequency. As long as  $\omega$  is far from any natural resonances [19] in the system the transfer function will be close to unity ( $\alpha_n \approx 1$ ).

To test Eqs. (3) and (5) we measure both the zeropressure current  $I_0$  and the current-pressure (I-P) relation, as a function of ac excitation. To measure  $I_0$  we use the fact that, in this type of cell,  $\phi$  exhibits periodic motion identical to a rigid pendulum [20,21]. For small amplitude pendulum oscillations, the angular frequency  $\omega_p$  becomes a direct measure of the critical current because  $\omega_p^2 \propto I_c$  [21]. Thus by recording the frequency of the small amplitude oscillations we determine the effective zero-pressure critical current  $I_0$ . We determine the frequency  $\omega_p$  by taking the Fourier transform of the low amplitude segment of the pendulum-mode motion of the membrane [21]. A typical Fourier transform is shown in the inset panel of Fig. 2(a). In this figure we plot the ratio  $I_0/I_c \equiv [\omega_p^2(P_{\rm ac})]/[\omega_p^2(P_{\rm ac}=0)]$  as a function of  $[(2m_3P_{\rm ac}/\rho)/(\hbar\omega)]$ . The solid line in this panel is the prediction for the zero-pressure mass current  $I_0/I_c$ . We can clearly see in Fig. 2(a) that  $I_0/I_c$  does indeed follow the prediction given by Eq. (5) for n=0.

The *I-P* characteristic at the dc pressures corresponding to Josephson frequencies satisfying Eq. (3) (with n > 0)

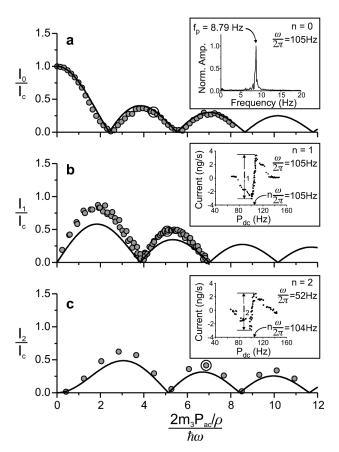


FIG. 2. (a) The n=0 case: A plot of the ratio  $I_0/I_c \equiv [\omega_p^2(P_{\rm ac})]/[\omega_p^2(P_{\rm ac}=0)]$  as a function of  $[(2m_3P_{\rm ac}/\rho)/(\hbar\omega)]$ . For n=0, the value of the transfer function  $P_{\rm ac}/P_V \equiv \alpha_0 =$ 1.25 is determined by requiring the zeros of our data to fit the zeros of the Bessel function  $J_0$ . The solid line in this panel is the prediction for the zero-pressure mass current  $I_0/I_c$ . We determine the frequency  $\omega_p$  by taking the Fourier transform of the low amplitude segment of the pendulum-mode motion of the membrane [21]. A typical Fourier transform of the pendulum mode is shown in the inset panel. (b) The n = 1 case: A plot of the current feature  $I_1/I_c$  as a function of  $[(2m_3P_{\rm ac}/\rho)/(\hbar\omega)]$ . The inset shows that the current feature occurs at  $\omega_J = \omega$  and indicates our definition of  $I_1$ . Fitting of the data to the  $J_1$  Bessel function zeros gives the value  $\alpha_1 = 1.16$ . (c) The n = 2 case: Similar to (b) except now  $\omega_i = 2\omega$ . Here  $\alpha_2 = 1.04$ . The double circles indicate the points derived from the raw data in each inset.

035301-2 035301-2

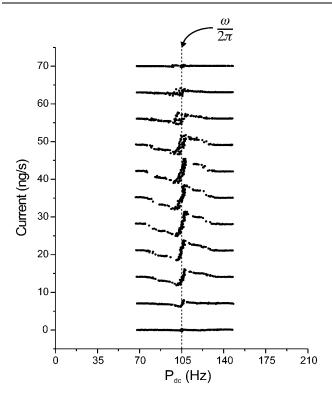


FIG. 3. A series of measured *I-P* curves, in a pressure range near  $\omega_J \approx \omega$ , for different values of the ac pressure amplitude. The horizontal axis represents dc pressure expressed in units of frequency  $f = 2m_3P_{\rm dc}/\rho h$ . The vertical axis is the mass current. The *I-P* curves are shifted upward from each other by a constant amount for clarity. Each shifted plot represents an increase in the ac pressure amplitude. The vertical line identifies  $\omega$ .

is directly measured using previously reported feedback techniques [18]. To fix  $P_{\rm dc}$ , the square of the feedback voltage to the lower diaphragm changes linearly in time at a rate proportional to the dc mass currents through the weak link. An absolute pressure calibration [12] combined with mass conservation allows us to convert the changing feedback voltage into a dc mass current measurement as a function of  $P_{\rm dc}$ .

To measure the new currents  $I_n$  for n>0 we select the dc pressure range corresponding to the frequency matching condition for a given  $\omega$  as in Eq. (3). We then measure the I-P characteristic for different values of  $P_{\rm ac}$ . In Fig. 3 we show a series of I-P curves as a function of increasing ac excitation. A sharp feature is quite apparent in the I-P curve when  $P_{\rm dc}$  corresponds to a Josephson frequency satisfying  $\omega_J=\omega$ . This figure shows that as  $P_{\rm ac}$  increases, the feature grows to a maximum and then decreases again to zero. Numerical solutions for the I-P characteristic in the presence of  $P_{\rm ac}$  for this type of experiment show a very similar feature.

Our definition for the magnitude of this feature  $I_1$  is shown in the inset of Fig. 2(b) and, when defined in this way, the numerical solution for  $I_1$  is found to satisfy Eq. (5). The measured magnitude  $I_1$  is plotted in 2(b) for

a wide range of  $P_{ac}$ . The  $J_1$  Bessel function dependence is clearly visible confirming Eq. (5) for n = 1.

A similar series of phenomena is observed when we measure the I-P curve at the second harmonic of external frequency or  $\omega_J = 2\omega$ . The data are shown in Fig. 2(c). Again, as  $P_{\rm ac}$  increases, the feature cycles through maxima separated by well-defined zeros as described by the  $J_2$  Bessel function. We did not extend the search of these phenomena to higher harmonics because the resonance structure of the cell becomes complicated [19].

In the frequency range of our experiment, the acinduced currents shown in 2(a)-2(c) are the *only* observed responses of the system to the ac excitation. The dc current changes occur only when  $\omega_J = n\omega$  and, in each case, they cycle in remarkable accordance with the appropriate Bessel function.

The striking agreement of the experiment with all aspects of the model [Eq. (1)–(5)] confirms the deep analogy between superfluid Josephson dynamics and the well-known dynamics of superconducting Josephson junctions. One significant aspect of these results is that it provides a stringent demonstration that a microaperture array is fully describable as a single superfluid weak link following Josephson's equations, removing any doubts on this issue [22]. These observations also open the way to potential applications of superfluid Josephson devices including a superfluid quantum pressure standard and a superfluid dc SQUID.

We acknowledge very helpful conversations with S. Vitale and assistance from S. Pereverzev, A. Loshak, and S. Backhaus with preliminary aspects of the experiment. This work was partially supported by the NSF Grant No. DMR-9807761, NASA Grant No. NAG8-1432, ONR Grant No. N00014-94-1-1008, and the Miller Institute for Basic Research (J. C. D.).

- [1] B. D. Josephson, Phys. Lett. 1, 251 (1962).
- [2] S. Shapiro, Phys. Rev. Lett. 11, 80 (1963).
- [3] P. W. Anderson and P. L. Richards, Phys. Rev. Lett. 14, 540 (1965).
- [4] D. R. Tilley and J. Tilley, Superfluidity and Superconductivity (Hilger, Bristol/New York, 1990), 3rd ed., pp. 282–290.
- [5] J. Parpia, Ph.D. thesis, Cornell University, 1979 (unpublished).
- [6] O. V. Lounasmaa et al., Phys. Rev. B 28, 6536 (1983).
- [7] K. K. Likharev, *Dynamics of Josephson Junctions and Circuits* (Gordon and Breach, New York, 1990).
- [8] C. C. Grimes, P. L. Richards, and S. Shapiro, J. Appl. Phys. 39, 3905 (1968).
- [9] B. N. Taylor, W. H. Parker, and D. N. Langenberg, Rev. Mod. Phys. 41, 375 (1969).
- [10] R. Pöpel, Metrologia 29, 153 (1992).
- [11] O. Avenel and E. Varoquaux, Phys. Rev. Lett. **60**, 416 (1988).
- [12] S. V. Pereverzev, A. Loshak, S. Backhaus, J. C. Davis, and R. E. Packard, Nature (London) **388**, 449 (1997).

035301-3 035301-3

- [13] A. Marchenkov, R. W. Simmonds, S. Backhaus, K. Shokhirev, A. Loshak, J. C. Davis, and R. E. Packard, Phys. Rev. Lett. 83, 3860 (1999).
- [14] D. Volhardt and P. Wolfle, *The Superfluid Phases of Helium-3* (Taylor & Francis, New York, 1990).
- [15] A recent experiment shows nonlinear effects in superfluid  $^4$ He interpreted as a  $\sin \phi$  current phase relation very close to  $T_{\lambda}$ . K. Sukhatme *et al.*, Nature (London) **411**, 280 (2001).
- [16] A. Amar, Y. Sasaki, R.L. Lozes, J.C. Davis, and R.E. Packard, J. Vac. Sci. Technol. B 11, 259 (1993).
- [17] H. J. Paik, J. Appl. Phys. 47, 1168 (1976).
- [18] S. Backhaus and R. Packard, in Proceedings of the 21st In-

- ternational Low Temperature Conference [Czech. J. Phys. **46**, 2743 (1996)].
- [19] R. W. Simmonds, A. Loshak, A. Marchenkov, S. Backhaus, S. Pereversev, S. Vitale, J. C. Davis, and R. E. Packard, Phys. Rev. Lett. 81, 1247 (1998).
- [20] H. Monien and L. Towordt, in *Proceedings of the Conference on Quantum Fluids and Solids, Banff, Alberta, Canada, 1986* [Can. J. Phys. **65**, 1388 (1987)].
- [21] A. Marchenkov, R. W. Simmonds, A. Loshak, J. C. Davis, and R. E. Packard, Phys. Rev. B 61, 4196 (2000).
- [22] O. Avenel, Yu. M. Mukharsky, and E. Varoquaux, Nature (London) 397, 484 (1999).

035301-4 035301-4